Vol. 5 (2012) *Acta Physica Polonica B Proceedings Supplement* No 2

RESULTS ON STRANGE RESONANCES IN Pb–Pb COLLISIONS AT $\sqrt{s_{NN}} = 2.76\,\mathrm{TeV}$ FROM THE ALICE EXPERIMENT AT THE LHC*

Christina Markert

for the ALICE Collaboration

The University of Texas, Austin, Texas, USA

(Received January 16, 2012)

Short lived hadronic resonances are sensitive to the properties of the medium created in a heavy-ion collision, in particular to the temperature, density and expansion velocity. Resonances decaying into hadrons are used to estimate the hadronic lifetime and hadronic interaction cross section in the hadronic phase between chemical and kinetic freeze-out. The detection of early decoupled resonances aims at studying chiral symmetry restoration via their mass shift and width broadening. There are reported the first $K^*(892)$ and $\phi(1020)$ results from Pb–Pb collisions at the LHC using the ALICE detector, with excellent identification of the decay particles in a large momentum range.

DOI:10.5506/APhysPolBSupp.5.243
PACS numbers: 21.65.Qr

1. Introduction

Hadronic resonances are sensitive to the transition, going from partons to hadrons, occurring in the fireball created by a heavy-ion collision. Chiral symmetry restoration is expected at the phase transition at a critical temperature of about $T_{\mathrm{c}} = 160\,\mathrm{MeV}$ [1]. The proposed signatures of chiral symmetry restoration for resonances are mass shifts and width broadenings. However, later interactions in the hadronic phase will contribute to the measured observables as well: the hadronic regeneration of resonances in the late hadronic medium will add resonances with vacuum properties, which do not show mass shifts or width broadenings. According to UrQMD calculations,

* Presented at the Conference “Strangeness in Quark Matter 2011”, Kraków, Poland, September 18–24, 2011.

the re-scattering of the resonance decay daughters and regeneration of resonances will change the measured yield predominantly in the low momentum region ($p_{\mathrm{T}} = 0$–$2\,\mathrm{GeV}/c$) [2]. Therefore, high-momentum resonances and their decay products are less likely to be affected by the hadronic medium. At RHIC energies of $\sqrt{s_{NN}} = 200\,\mathrm{GeV}$, the lifetime of the hadronic phase $\Delta\tau > 4\,\mathrm{fm}/c$ is derived from resonance measurements [3, 4]. The assumption is made that the chemical freeze-out occurs at hadronisation. Although they are not discussed here, leptonic decays are more sensitive probes for chiral symmetry restoration due to the small interaction cross section of the decay daughters with the hadronic medium. The leptonic decays allow us to reconstruct resonances from earlier decay. The high-momentum resonances ($p_{\mathrm{T}} > 2\,\mathrm{GeV}/c$) are also sensitive probes of chiral symmetry restoration due to the lower interaction rates of the decay hadrons with the hadronic medium. A more detailed selection of resonances can be done via a jet-triggered analysis to select for longer path lengths through the medium, *i.e.* the selection of resonances from the away-side distribution of a triggered di-jet or leading particle [5]. This removes from consideration resonances created close to the surface of the interaction region, which have predominately vacuum properties. This newly suggested analysis requires a large jet production cross section and profits from a longer partonic lifetime (expected to be $\sim 10\,\mathrm{fm}/c$ at LHC). ALICE is the optimal detector for such a study since it provides excellent particle identification capabilities for decay particles and provides jet identification via leading particle selection or full jet reconstruction using the Electromagnetic Calorimeter (EMCal) [6] in addition. Preliminary results from the first Pb–Pb run in 2010 are reported.

2. Resonance reconstruction

The main ALICE detector components used to identify charged hadrons are the Time Projection Chamber (TPC) [7], the Inner Tracking System (ITS) [8] and the Time-of-Flight detector (TOF). The TPC and ITS are used to measure particle momenta and reconstruct the main vertex position. In this analysis, the position of the vertex is restricted to be within 10 cm of the centre of the ALICE detector. In the TPC, the particles are measured over the pseudorapidity range $|\Delta\eta| < 0.9$. Resonances are identified by reconstructing their invariant mass through their hadronic decays: specifically, $K^*(892) \rightarrow \pi^{\pm} + K^{\mp}$ and $\phi(1020) \rightarrow K^{\pm}K^{\mp}$. The decay daughters are identified using TPC energy loss (at low p_{T}) and their speed measured by the Time-of-Flight detector (for $p_{\mathrm{T}} > 0.7\,\mathrm{GeV}/c$) [9,10]. Uncorrelated hadron pairs form a large background to the resonance signal. The background in Pb–Pb collisions is calculated via the mixed event technique and subtracted from the signal histogram.

3. Resonance mass and width

The $K + \pi$ invariant mass distribution in the range $p_{\rm T} = 2$–$2.5\,{\rm GeV}/c$ is shown in figure 1 (left) for the 0–20% most central Pb–Pb collisions at $\sqrt{s_{NN}} = 2.76\,{\rm TeV}$. The corresponding signal from a HIJING simulation including the ALICE detector acceptance is shown in figure 1 (right). The extracted mass and width from a Breit–Wigner fit to the signal is shown as functions of $p_{\rm T}$ in figure 2. In the low momentum region ($p_{\rm T} < 2\,{\rm GeV}/c$), the measured masses are lower than expected from simulation, which includes the PDG values (vacuum properties). However, we observe a similar mass shift in p–p collisions, which indicates that this is not a medium effect.

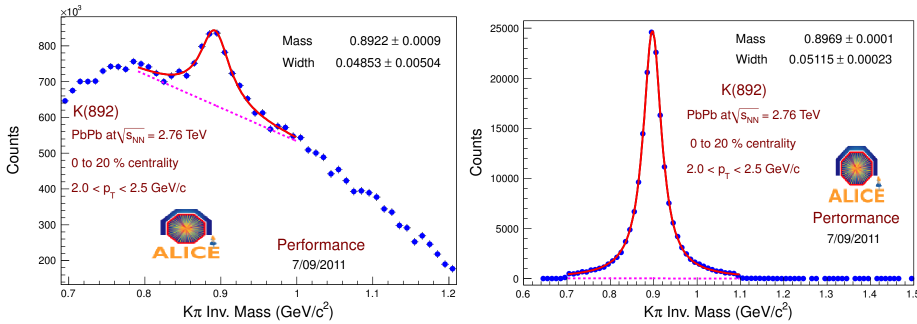

Fig. 1. Left: $K + \pi$ invariant mass spectrum between $p_{\rm T} = 2$–$2.5\,{\rm GeV}/c$ in Pb–Pb collisions at $\sqrt{s_{NN}} = 2.76\,{\rm TeV}$ after subtraction of the mixed event background. The mass and width were extracted from a Breit–Wigner function fit to the signal plus a straight line fit to the residual background. Right: $K^*(892)$ $(K + \pi)$ invariant mass spectrum between $p_{\rm T} = 2$–$2.5\,{\rm GeV}/c$ from HIJING simulation of Pb–Pb collisions at $\sqrt{s_{NN}} = 2.76\,{\rm TeV}$. The mass and width are extracted from a Breit–Wigner fit to the signal.

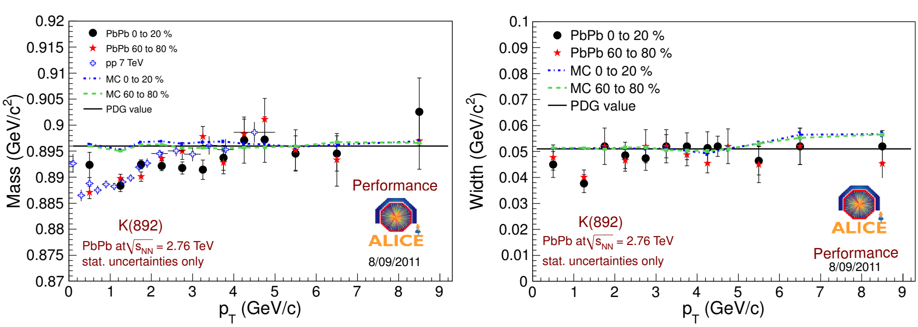

Fig. 2. Mass and width of $K^*(892)$, extracted from Breit–Wigner function fits, *versus* momentum for different collision systems and a HIJING simulation. The measurements include the statistical uncertainties only.

Above $p_{\mathrm{T}} > 2\,\mathrm{GeV}/c$, the measured mass is consistent with the simulation and the PDG value. The measured width is in agreement with the expected value derived from the simulation throughout the whole momentum range. The measurements include the statistical uncertainties only. The fluctuation of one bin at $p_{\mathrm{T}} = 1\,\mathrm{GeV}/c$ indicates a systematic uncertainty of about 10–15% on the width.

4. Hadron–resonance correlation

Figure 3 shows the invariant mass distribution of $\phi(1020)$ (for $p_{\mathrm{T}} > 1.5\,\mathrm{GeV}/c$) in p–p (left) and Pb–Pb (right) collisions; each event includes a trigger hadron with $p_{\mathrm{T}} > 3\,\mathrm{GeV}/c$. Charged hadron *vs.* $\phi(1020)$ angular correlations are shown in figure 4 for $\sqrt{s} = 7\,\mathrm{TeV}$ p–p collisions (left) and the corresponding PYTHIA simulation (right), which includes the effects of the ALICE detector acceptance and efficiencies. The angular correlation ($\Delta\phi$) clearly shows a near- and away-side distribution of the correlated resonance with respect to a higher momentum trigger particle. The width of the near-side peak is about 25–30% larger in the data than in the PYTHIA simulation, while the widths of the away-side peaks are in agreement within statistical uncertainties. The angular correlation ($\Delta\phi$) in Pb–Pb (figure 5) indicates a broader width on the near-side than predicted by HIJING and PYTHIA. Due to the low statistics we are not able to draw any conclusions from the away-side distribution yet.

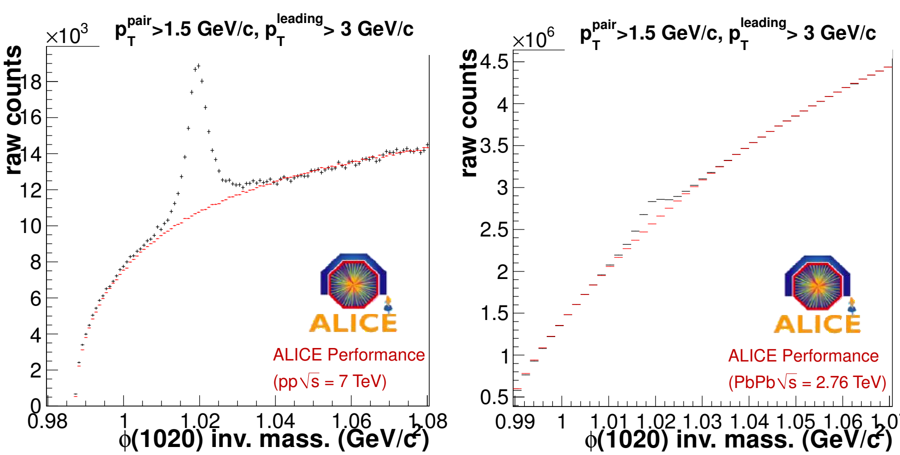

Fig. 3. Invariant mass distribution of K^+ and K^- pairs showing the $\phi(1020)$ signal for $p_{\mathrm{T}} > 1.5\,\mathrm{GeV}/c$ in 160 million p–p events at $\sqrt{s} = 7\,\mathrm{TeV}$ (left) and 16 million Pb–Pb events at $\sqrt{s}_{NN} = 2.76\,\mathrm{TeV}$ (right).

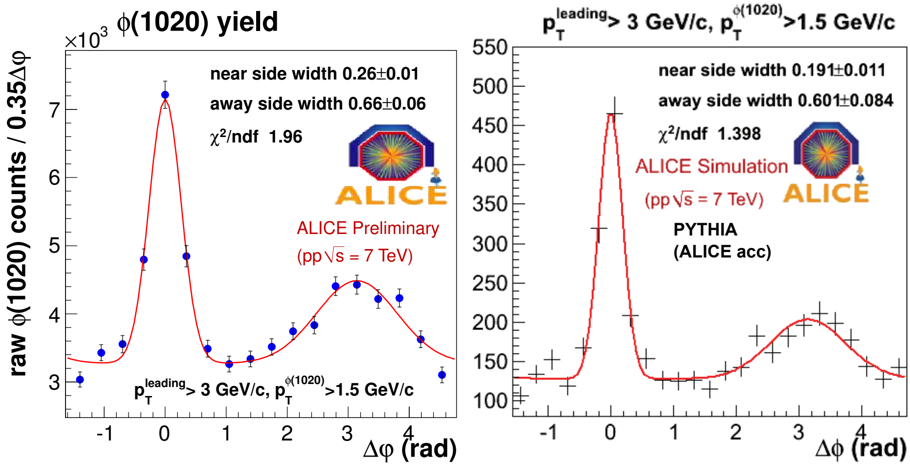

Fig. 4. Charged hadron *vs.* $\phi(1020)$ resonance angular correlations with hadron trigger $p_{\mathrm{T}} > 3\,\mathrm{GeV}/c$ and associated $\phi(1020)$ $p_{\mathrm{T}} > 1.5$ GeV/c for $\sqrt{s} = 7\,\mathrm{TeV}$ p–p collisions normalized to the number of triggers (left) and the corresponding PYTHIA simulation including the ALICE acceptance and efficiencies (right).

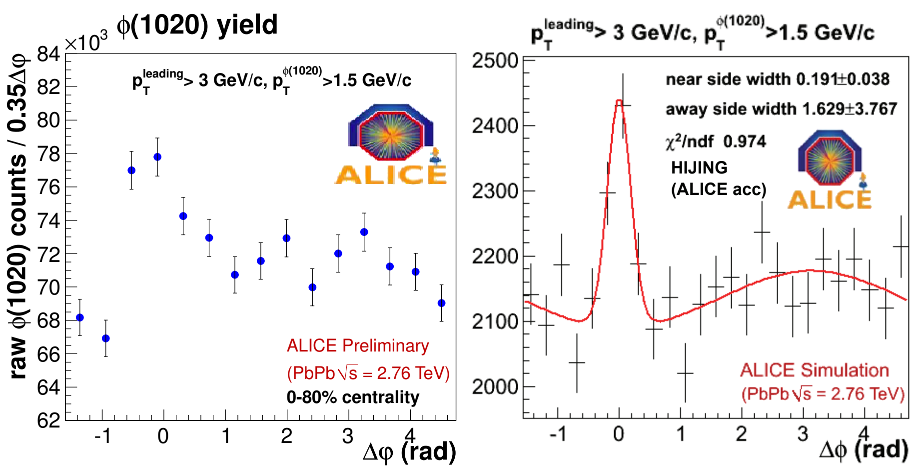

Fig. 5. Charged hadron *vs.* $\phi(1020)$ resonance angular correlations with hadron trigger $p_{\mathrm{T}} > 3\,\mathrm{GeV}/c$ and associated $\phi(1020)$ $p_{\mathrm{T}} > 1.5\,\mathrm{GeV}/c$ for $\sqrt{s}_{NN} = 2.76\,\mathrm{TeV}$ Pb–Pb collisions normalized to the number of triggers (left) and the corresponding HIJING simulation including the ALICE acceptance and efficiencies (right).

The mass and width of the $\phi(1020)$ are constant over the full $\Delta\phi$ range in Pb–Pb (figure 6). The near-side peaks are used as reference data to cancel out detector effects on the mass shift and width broadening. We do not observe a mass and width modification in the given momentum region. However, this result is expected since the number of resonances from jets is about 10% of the number of resonances from the background. This analysis needs more statistics of higher momentum resonances to enrich the contributions from jets.

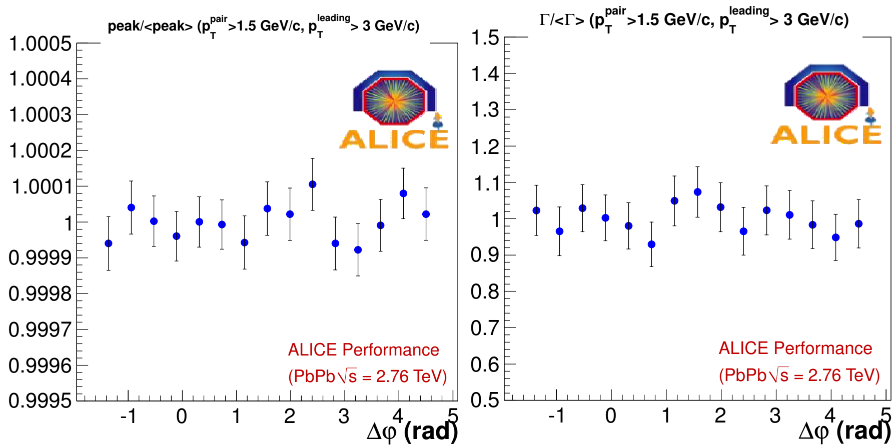

Fig. 6. Normalized mass and width of the $\phi(1020)$ ($p_{\mathrm{T}} > 1.5\,\mathrm{GeV}/c$) *versus* the azimuthal angle with respect to the trigger particle ($p_{\mathrm{T}} > 3\,\mathrm{GeV}/c$) in $\sqrt{s}_{NN} = 2.76\,\mathrm{TeV}$ Pb–Pb collisions.

This work was supported by the U.S. Department of Energy Office of Science under contract number DE-SC0003892.

REFERENCES

[1] Y. Aoki *et al.*, *Phys. Lett.* **B643**, 46 (2006); *J. High Energy Phys.* **0906**, 088 (2009); S. Borsanyi *et al.*, *J. High Energy Phys.* **1009**, 073 (2010).

[2] M. Bleicher *et al.*, *Phys. Lett.* **B530**, 81 (2002) and private communication.

[3] B.I. Abelev *et al.* [STAR Collaboration], *Phys. Rev. Lett.* **97**, 132301 (2006).

[4] G. Torrieri *et al.*, *Phys. Lett.* **B509**, 239 (2001).

[5] C. Markert, R. Bellwied, I. Vitev, *Phys. Lett.* **B669**, 92 (2008).

[6] ALICE EMCal Physics Performance Report (2010), `arXiv:1008.0413v1 [physics.ins-det]`.

[7] J. Alme *et al.*, *Nucl. Instrum. Methods Phys. Res.* **A622**, 316 (2010).

[8] K. Aamodt *et al.* [ALICE Collaboration], *JINST* **5**, P03003 (2010).

[9] ALICE Collaboration, *JINST* **3**, S08002 (2008).

[10] A. Pulvirenti [ALICE Collaboration], *Nuovo Cim.* **C34**, 141 (2011).